Journal of Biomolecular NMR, **23:** 139–150, 2002.
KLUWER/ESCOM

Interpretation of ^{15}N NMR relaxation data of globular proteins using hydrodynamic calculations with HYDRONMR

Pau Bernadó[a], José García de la Torre[c] & Miquel Pons[a,b,*]
[a]*Departament de Química Orgànica, Universitat de Barcelona, Martí Franquès, 1-11, 08028-Barcelona, Spain;*
[b]*Laboratori de RMN de Biomolècules, Parc Científíc de Barcelona, Josep Samitier 1-5, 08028-Barcelona, Spain;*
[c]*Departmento de Química Física, Facultad de Química, Universidad de Murcia, 30071-Murcia, Spain*

Received 28 February 2002; Accepted 17 April 2002

Key words: aggregation, anisotropy, exchange, hydrodynamic calculations, protein dimer, protein NMR, relaxation, rotational diffusion

Abstract

HYDRONMR is an implementation of state of the art hydrodynamic modeling to calculate the spectral density functions for NH or C^{α}-H vectors in a rigid protein structure starting from an atomic level representation. Thus HYDRONMR can be used to predict NMR relaxation times from a rigid model and to compare them with the experimental results. HYDRONMR contains a single adjustable parameter, the atomic element radius. A protocol to determine the value that gives the best agreement between calculated and experimental T_1/T_2 values is described. For most proteins, the value of the atomic element radius ranges between 2.8 Å and 3.8 Å with a distribution centered at 3.3 Å. Deviations from the usual range towards larger values are associated to aggregation in several proteins. Deviations to lower values may be related to large-scale motions or inappropriate model structures.
If the average structure is correct, deviations between experimental T_1/T_2 values and those calculated with HYDRONMR can be used to distinguish residues affected by anisotropic motion from those that are involved in chemical exchange.

Introduction

Protein function is intrinsically related with its dynamic behavior (Feher and Cavanagh, 1999). Relevant dynamic processes include fast local fluctuations and large amplitude motions of domains or secondary structure fragments. Nuclear magnetic resonance, through relaxation experiments, is a powerful tool for the quantitative study of motions in a wide range of time scales (Palmer III et al., 1996; Dayie et al., 1996; Fischer et al., 1998). Relaxation rates are usually interpreted using the so-called model free approach (Lipari and Szabo, 1982), where local fluctuations, described by the order parameter S^2, are considered to be independent of the reorientation of the whole molecule, described by a global correlation time τ_c. Chemical exchange processes provide an additional contribution to relaxation. While local effects provide the most chemically relevant information, e.g. entropy estimates from S^2 (Akke et al., 1993; Yang and Kay, 1996; Spyracopoulos and Sykes, 2001) or kinetic constants from exchange contributions (Mulder et al., 2001), global tumbling in general dominates all relaxation measurements. Moreover, most proteins are anisotropic to some degree and differences in relaxation rates between residues due to this effect are often comparable to those arising from chemical exchange and fast local motions. Sorting out the different, sometimes competing, contributions is an essential step for the correct analysis of relaxation data. Considering that a structural model is often available before relaxation studies are initiated, state of the art hydrodynamic calculations may provide a way to account for the contributions to relaxation arising from rotational diffusion.

*To whom correspondence should be addressed. E-mail: mpons@qo.ub.es

The link between structural and dynamic information provided by hydrodynamic calculations allows also the use of relaxation information to test the validity of structural models. The precision of structures derived from NMR has increased in the last years due to the incorporation of long range information from dipolar couplings (Tolman et al., 1995; Tjandra and Bax, 1997) and relaxation data (Tjandra et al., 1997; Tsan et al., 2000). In both types of experiments, long range information is derived from the orientation of bond vectors, that may be located far apart in the protein, with respect to the axes of a unique tensor describing the alignment properties or the rotational diffusion of the complete structure.

The global tensors are not known *a priori* but are optimized during the structure determination process to maximize the internal consistency of the complete set of experimental data under the implicit assumption that the global structure can be considered invariable in the relevant time scales. This assumption may not always be fulfilled, especially in large multi-domain proteins that might be involved in large amplitude motions, or in cases where there is dynamic microaggregation or oligomerization under the NMR experimental conditions. These effects may easily go undetected and the validity of the resulting structural model should be validated by back calculation of the long-range NMR observables.

Programs that calculate the steric alignment tensor and the expected dipolar couplings from the three dimensional structure of a protein are already available (Zweckstetter and Bax, 2000; Fernandes et al., 2001). Global tumbling is characterized by the rotational diffusion tensor that can be calculated from hydrodynamic principles.

In this communication we present a comparison of the T_1/T_2 values predicted by HYDRONMR (García de la Torre et al., 2000b) with published experimental data for a variety of proteins. Although HYDRONMR calculates spectral density functions, $J(\omega)$ from which all relaxation parameters can be computed, following the established practice we have concentrated our analysis in the ^{15}N T_1/T_2 ratios. To a good approximation, T_1/T_2 ratios are not affected by rapid internal motions or by the magnitude of the chemical shift anisotropy (Tjandra et al., 1995). From this comparison we conclude that, in general, there is a good agreement between experimental relaxation values and those calculated using HYDRONMR and the 3D structures using an atomic element radius that range from 2.8 to 3.8 Å. Substantial deviations from these values suggest the presence of underlying dynamic processes or aggregation. On the other hand, local deviations between experimental and calculated values can be usually related to chemical exchange or fast internal motions and may provide a tool to select residues that provide a faithful report of the overall tumbling, needed to extract local dynamic information from relaxation data.

Hydrodynamic calculations using simpler bead models have been compared in the past with experimental relaxation data from individual proteins (Tjandra et al., 1995; Mackay et al., 1998; Cordier et al., 1998; Osborne and Wright et al., 2001). Krishnan and Cosman have calculated rotational correlation times for 75 proteins (Krishnan and Cosman, 1998). Some of these calculations used a computational tool that implements our old HYDRO program for a calculation that is done directly on a primary bead method (Orekhov et al., 1995). This procedure has known problems that are avoided using the bead shell modeling methodology.

Methods

HYDRONMR

Starting from the seminal work of Bloomfield and García de la Torre (García de la Torre and Bloomfield, 1977, 1981) the so called bead methods have been used to derive the hydrodynamic properties of objects of arbitrary shapes. For a recent review of theory and methodology, see Carrasco and García de la Torre (1999) Of these, the bead shell methods offer, with a moderate expense in computing time, the most accurate hydrodynamic calculations. The application of these methods to the study the hydrodynamic properties of molecules represented at the atomic level has been critically reviewed (García de la Torre et al., 2000a). An optimized protocol has been implemented in the HYDRONMR program (García de la Torre et al., 2000b), which is included in the HYDRO suite of programs (see Computer programs section).

HYDRONMR uses a shell model (Filson and Bloomfield, 1967), which is constructed from the atomic representation of the protein contained in a PDB file. Initially, each nonhydrogen atom is replaced by a spherical element of radius *a*, which we call the atomic element radius, to yield a primary hydrodynamic model. The shell model is then obtained from the primary hydrodynamic model by representing its

surface by a set of tangent beads of radius σ. Hydrodynamic properties are calculated for decreasing values of σ and extrapolated to $\sigma = 0$. As described elsewhere (Carrasco and García de la Torre, 1999), this procedure avoids the bead overlap problems present in the primary hydrodynamic models that can cause severe problems in the description of the hydrodynamic interactions and in the volume correction. The atomic element radius is the only adjustable parameter of the model. A lower bound for this radius should be the van der Waals radii of the atoms but larger values are expected due to the neglect of hydrogen atoms and the effect of the hydration shell. The choice of the *a* value has a strong influence in the global size, and therefore in the correlation time but has negligible effects on the shape of the model and therefore on the orientation of the tensor axes with respect to the protein fixed reference frame. As a consequence, the relaxation times computed for individual residues with different values of *a* are just scaled.

Choice of the atomic element radius a

HYDRONMR calculations assume a rigid model relaxing only through dipole-dipole and chemical shift anisotropy mechanisms. A comparison between calculated and experimental data has to be restricted to those residues that are not affected by large amplitude or very fast internal motions or by chemical exchange.

Selection of the set of residues that genuinely report on the overall tumbling of the protein is a crucial problem in the analysis of relaxation data and often involves some implicit *a priori* assumptions about the global shape and global dynamic behavior of the protein. Different filtering strategies have been suggested to avoid introducing biases in the selection of residues that could introduce errors in the characterization of the global tumbling properties of the protein.

For data measured at a single magnetic field, the filtering protocol of Tjandra et al. is often used (Tjandra et al., 1995), an improved, two stage filter, has been recently suggested (Pawley et al., 2001). It has been pointed out, however, that the residues more affected by anisotropic tumbling may be wrongly assigned as experiencing conformational exchange and eliminated. This would skew the estimation of the global tumbling towards a more isotropic model (Kroenke et al., 1998; Fushman et al., 2000) because the probability of finding residues oriented towards the main axes of the diffusion tensor is very low. Detection of exchanging residues can also be accomplished when other experimental measures are available. This is the case of H-^{15}N/^{15}N CSA relaxation interference, which is insensitive to chemical exchange (Kroenke et al., 1998), or use of RDC in an sterical orienting media, provided by the fact that orienting and rotational diffusion tensors are almost equivalent (de Alba et al., 1999).

Our approach is shown schematically in Figure 1. We start from a three dimensional structure that allows the calculation of the global tumbling contribution to relaxation for each residue. Individual residues affected by exchange or very fast motion would appear as outliers in the fit of calculated versus observed values. However, in order to do that, we have to choose the value of the atomic element radius, *a*, which best reproduces the observed T_1/T_2 values of residues not affected by exchange. Fortunately, numerical results have shown that the relative deviations of T_1/T_2 for a residue *i*, ∇_i,

$$\nabla_i = \frac{((T_1/T_2)_i - \langle T_1/T_2 \rangle)}{\langle T_1/T_2 \rangle},$$

from the average of T_1/T_2 values over all residues in the protein, $\langle T_1/T_2 \rangle$, are remarkably insensitive to the value of a. Therefore, in order to select which residues have to be included in the optimization of the atomic element radius we compare experimental and calculated ∇_i values and remove those residues with absolute deviations higher than a threshold. For a given threshold, F, which is a fraction of the standard deviation, SD, of the experimental ∇_i values, the a value is chosen so that the error function, χ^2,

$$\chi^2 = \sum_i \frac{[(T_1/T_2^{exp_i} - (T_1/T_2)_i^{calc}]^2}{E(T_1/T_2)_i^{exp^2}},$$

for the retained residues is minimized, where $E(T_1/T_2)^{exp_i}$ is the experimental error in T_1/T_2 ratio for residue *i*. The actual threshold is determined by the value at which a further reduction does not lead a change in the optimum value of *a*.

Results and discussion

Table 1 shows the calculated and reported values of the global rotational diffusion tensor for 15 proteins for which extensive relaxation data are available in the literature. Table 1 includes the value of the atomic element radius *a* that best reproduces the reported T_1/T_2 values. An excellent agreement is observed between calculated and τ_c and D_{par}/D_{per} values derived directly

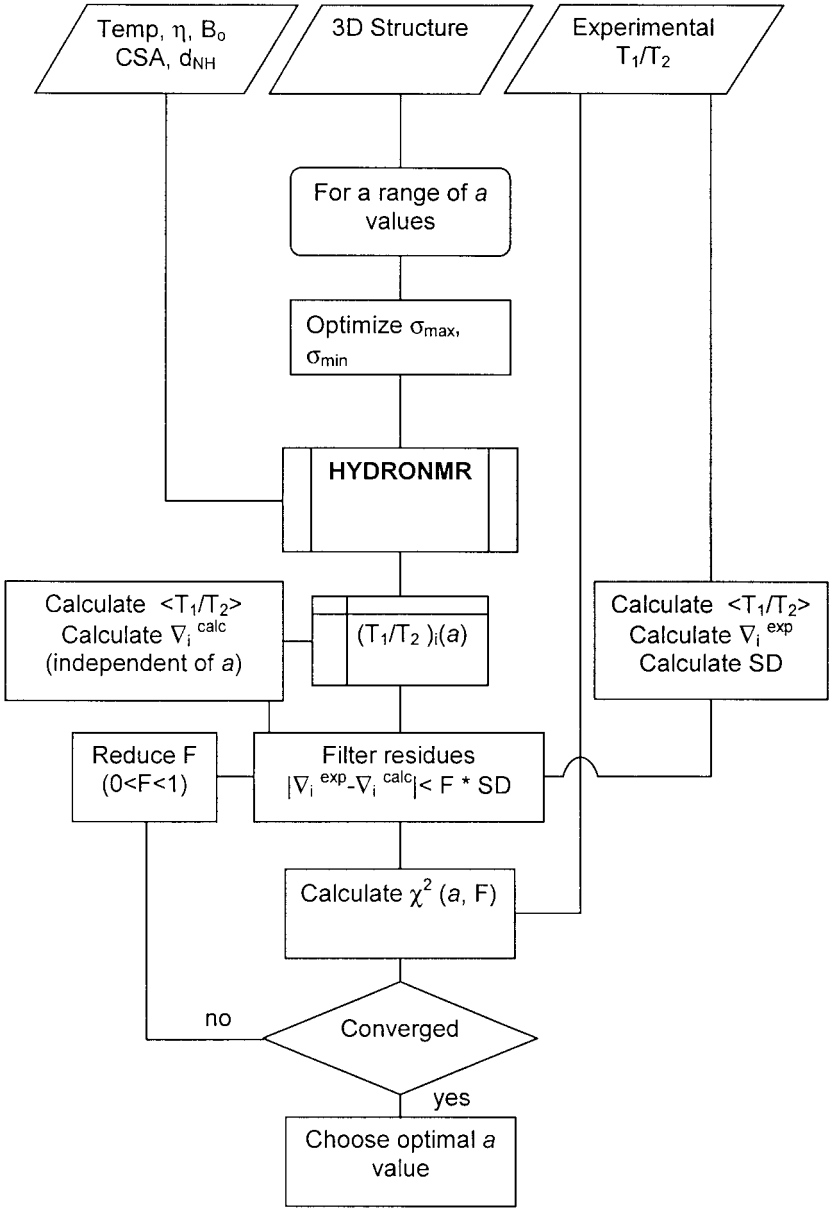

Figure 1. Flow-chart of the procedure used to select the optimal *a* value.

from the experimental data using standard procedures. Figure 2 shows plots of calculated versus experimental values of T_1/T_2 for four proteins (HIV-protease, Barnase, Ribonuclease H and Outer Surface Protein) that demonstrate that HYDRONMR also reproduces correctly the effects of global motion on individual residues of rigid anisotropic proteins.

In a previous work (García de la Torre et al., 2000b) we had determined the *a* values that give the best fit to the experimental correlation times for a series of 15 proteins taken from the extensive compilation of Krishnan and Cosman (Krishnan and Cosman, 1998). This compilation is focused in isotropic globular proteins that exist in a single oligomeric state (monomer or dimer). We found an average value of 3.2 Å with an average of the absolute deviation from experimental values of 9%. In the present study, using an optimization protocol that uses directly the experimental T_1/T_2 values we find an average value of a of 3.4 Å with an average absolute deviation between

Table 1. Experimental and calculated hydrodynamic parameter

Protein[a]	PDB	*a* (Å)	τ_c (ns) Calcul.	τ_c (ns) Exper.	D_{par}/D_{per} Calcul.	D_{par}/D_{per} Exper.	Reference[d]
Troponin C	5tnc	3.30	4.71	4.86	1.06	1.10	Gagné et al., 1998
Enzyme I N-termn[e]	1zym	3.70	13.3	13.1	1.81	2.1	Tjandra et al., 1997
Ribonuclease H[f]	2rn2	3.00	9.77	9.75[f]	1.24	1.23	Kroenke et al., 1999
SpoOf	2fsp	3.30	8.14	7.72	1.20	*isotropic*	Feher and Cavanagh, 1999
Ubiquitin	1ubq	2.20	4.06	4.11	1.43	1.16	Tjandra et al., 1995
Ubiquitin 1-73	1ubq	3.05	3.97	4.11	1.17	1.16	Tjandra et al., 1995
HIV-protease dimer	1bvg	2.80	10.63	10.65	1.51	1.34	Tjandra et al., 1996
Outer surface protein	1osp	2.95	13.32	13.7	2.37	2.12	Pawley et al., 2001
Antifungal protein 1	1gh5	4.35	8.05	8.05	1.27	1.18	Campos-Olivas et al., 2001
Cytochrome c'[g]	1rcp	4.35	9.27	9.63	1.50	1.39	Tsan et al., 2000
Cytochrome c_2[g]	1c2r	4.40	10.34	10.41	1.33	1.23	Blackledge et al., 1998
Barnase	1a2p	3.50	5.02	4.99	1.33	1.1	Sahu et al., 2000
Barstar C40.82A	1bta	4.40	5.95	5.7	1.15	*isotropic*	Wong et al., 1997
Barnase/barstar	1brs	4.25	9.68	9.46	1.46	1.26	Sahu et al., 2000
Titin I27	1tit	3.05	5.96	5.75	1.61	*isotropic*	Improta et al., 1998
Titin I28[h]	model	4.10	6.77	6.55	1.74	*isotropic*	Improta et al., 1998

[a]All calculations were done using a N-H distance of 1.04 Å and a ^{15}N CSA of -160.0 ppm (Case, 1999). Calculations were performed using the experimental temperature and the corresponding viscosity. Hydrogen atoms were added to X-ray structures using INSIGHT II (MSI).
[b]Calculated as $D_z/(0.5(D_x + D_y))$.
[c]Published values obtained by fitting to an axially symmetric or isotropic model, except for 1bvg and 1c2r that were fitted to a completely anisotropic model.
[d]Source of the experimental NMR relaxation data.
[e]Structural data is only available for residues 3–249. Relaxation data are from the complete protein (residues 1–259).
[f]Data at 14.1 T. Anisotropy derived from analysis of η_{xy}/η_z at 11.74 T (Kroenke et al., 1999).
[g]Monomer structure.
[h]Homology model based on the structure of I27 used in a Titin 1 model (Improta et al., 1996).

the calculated and observed τ_c values of 4.3%. In a separate study using the same methodology, an average value of 3.3 Å was found to give the optimal fit to hydrodynamic properties including translational diffusion, sedimentation coefficients, rotational diffusion and intrinsic viscosity of a different set of proteins (García de la Torre et al., 2000a; García de la Torre, 2001). A similar range of values has been obtained for small nucleic acids (Fernandes et al., 2002).

Thus, four separate studies using the same methodology but focussing in different hydrodynamic properties or using different optimization protocols converge to the same optimal value for the atomic element radius of 3.3 Å. In all the studies, however there is significant dispersion in the optimal values for different proteins with individual values covering the range from 2.6 to 4.8 which amount to maximal individual deviations from the mean of -21% and $+45\%$, respectively.

Krishnan and Cosman observed a similar dispersion in the deviations of the τ_c values calculated with a fixed radius around the experimental ones with maximal deviations of $+13\%$ and -35%. These authors ascribed the dispersion to departures from the isotropic model used in most of the early estimates of correlation times from experimental data. Indeed, severe errors in the estimation of the correlation time are introduced when a moderately anisotropic protein, $D_{par}/D_{per} > 1.2$, is assumed to be isotropic (Korzhnev et al., 2001). However, in the present survey, the optimization of the *a* value has been performed using the experimental raw T_1/T_2 values and anisotropy effects are included in the optimization.

An additional source of dispersion could be individual variations in the hydration degree of different proteins. However, we have not found any correlation between the optimal *a* value and the percentage of charged residues in the sequence that, *a priori*, would be the most obvious source for differential hydration. The expected accuracy in the estimation of the hydration layer, assuming that the temperature is known to $\pm$ 0.2 K, can be taken as an estimation of the maximal

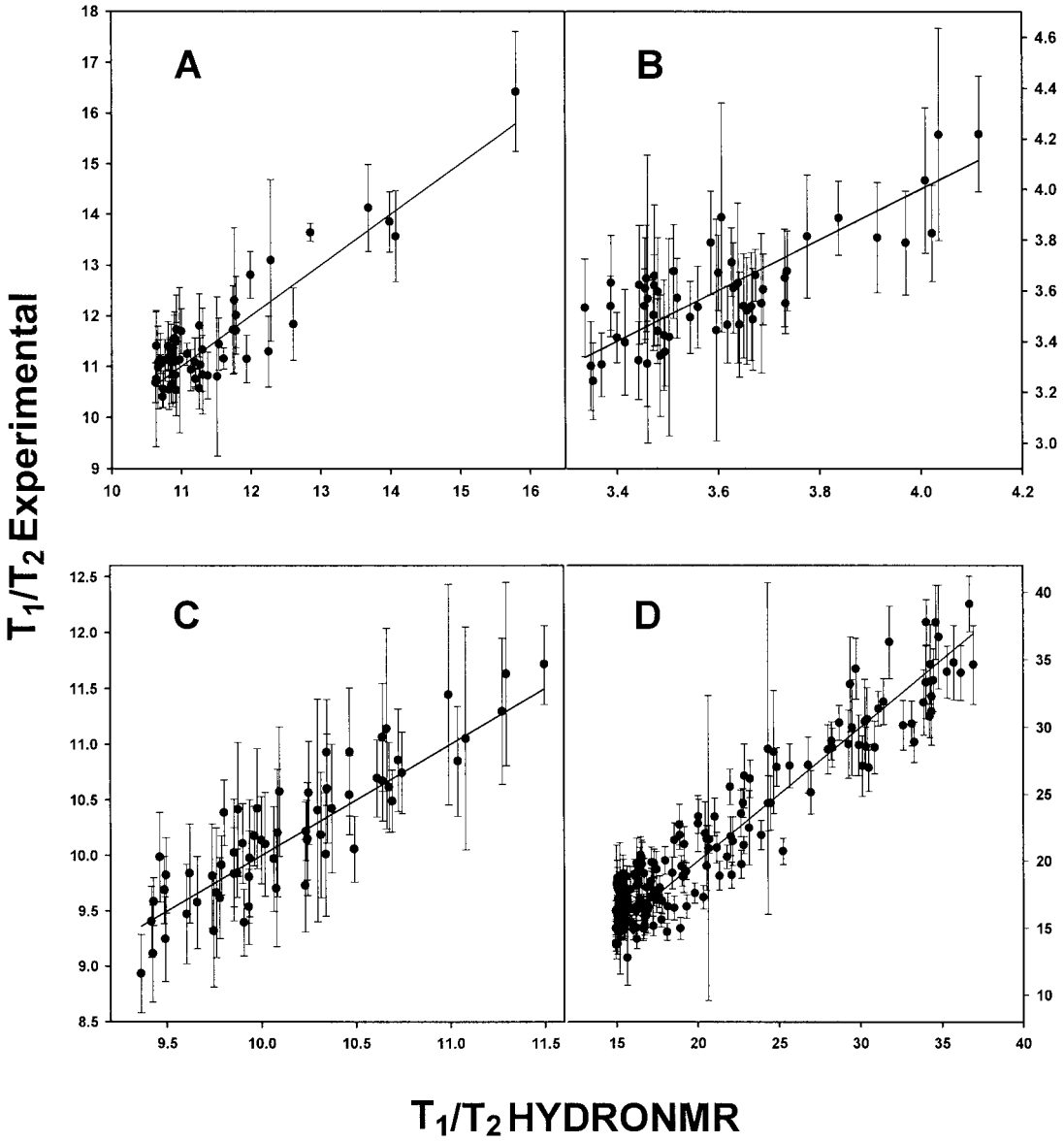

Figure 2. Comparison between experimental and HYDRONMR calculated values of T_1/T_2 for (A) HIV-protease, (B) Barnase, (C) Ribonuclease H at 14.1 T, (D) OspA. Experimental values where filtered with 0.7 times the standard deviation of ∇ as explained in the text. The sources of experimental data are referenced in Table 1.

accuracy of the atomic element radius and is ±0.2 Å (García de la Torre, 2001). Thus, fluctuations of a outside 3.3 ± 0.2 Å should be investigated. Analysis of individual proteins that require extreme values of a to fit the experimental relaxation data may indicate additional sources of variability, that may confer some diagnostic value to the a parameter.

Six proteins in Table 1 need a values higher than 4 Å: Barstar, Barnase-Barstar complex, cytochrome c', cytochrome c_2, Titin module 128 and antifungal protein 1. Barstar, which exists as a dimer in the crystal form, has been recently shown to be involved in a monomer-dimer equilibrium in solution (Korchuganov et al., 2001). This is reflected in the exchange detected in some residues involved in the dimerization face of barstar (Wong et al., 1997). The dimerization interface is opposite to the barnase binding loop and concentration dependent line widths have been observed in the dimerization interface of Barstar in the Barnase–Barstar complex, suggesting

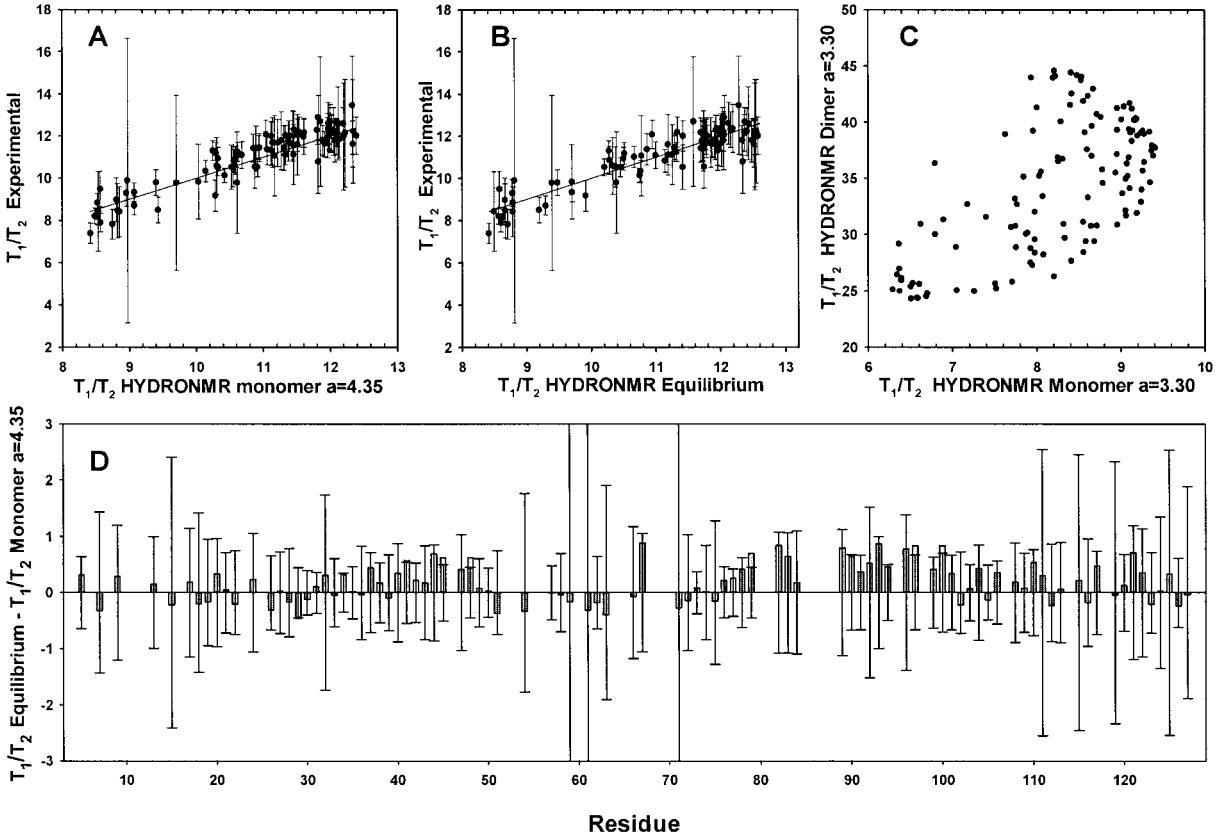

Figure 3. Comparison of the highly hydratated monomer and dimer-monomer equilibrium scenarios for cytochrome c'. (A) Comparison of experimental and HYDRONMR calculated T_1/T_2 values for cytochrome c' monomer with $a = 4.35$ Å. (B) Comparison between experimental and predicted T_1/T_2 values with a population of monomer of 0.80, using a value of $a = 3.30$ Å for both monomer and dimer. Straight lines in (A) and (B) have slope 1. (C) Plot of calculated T_1/T_2 values for equivalent residues in monomer and dimer with $a = 3.30$ Å. (D) Difference between calculated T_1/T_2 using the two models. Error bars correspond to the experimental uncertainty of T_1/T_2 values. Only residues retained by the filtering protocol explained in the text are plotted.

that the complex also partially dimerizes in solution. It is reassuring that the relaxation data of Barnase, in the absence of Barstar, are well reproduced by HYDRONMR with an a value of 3.5 Å.

Both cytochrome c' and cytochrome c_2 need very high values of a to reproduce the measured relaxation rates. Both proteins crystallize as dimers. However, using extensive, high quality, relaxation data, Tsan and collaborators (Tsan et al., 2000) concluded that cytochrome c' was present as a monomer in solution at the 7 mM concentration used, based on the agreement between the optimal rotational diffusion tensor and the inertia tensor of the monomer. The conclusion was supported by the results of hydrodynamic calculations of relaxation parameters using the monomer structure and a primary bead method. However, very large hydration shell (3 Å) was needed, in contrast to recent findings suggesting that protein hydration shells are around 1.2 Å wide (García de la Torre, 2001). Likewise, cytochrome c_2 relaxation data (Cordier et al., 1998) were subjected to a careful analysis, including anisotropic motion, based on the assumption of a monomeric structure (Blackledge et al., 1998).

A previous study suggested a monomer/dimer equilibrium for cytochrome c' in solution (Cusanovich, 1971). As pointed out previously, fast exchange between two species on the NMR-relaxation timescale, would cause an averaging of the relaxation matrix and, as a consequence, a monoexponential decay in the T_1 and T_2 experiments, so the equilibrium could remain undetected (Fushman et al., 1997). This situation would lead to apparent ^{15}N relaxation rates, R_1^{app} and R_2^{app}:

$$R_1^{app} = p_M R_1^M + (1 - p_M) R_1^D,$$
$$R_1^{app} = p_M R_2^M + (1 - p_M) R_2^D + R_{ex},$$

where P_M is the population of the monomeric specie and M and D refer to the monomer and dimer, respectively. R_{ex} in the fast exchange limit is given by

$$R_{ex} = p_M(1 - p_M)\Delta\omega^2/k_{ex},$$

where $\Delta\omega$ is the chemical shift difference between the two sites and k_{ex}, is the sum of the direct and reverse pseudo-first order rate constants. For weak complexes (K_d in the mM range) k_{ex} is large and contributions to R_{ex} from the dimerization process are expected to be negligible. Furthermore, residues with detectable exchange contributions are removed by our protocol.

In order to check if a monomer/dimer equilibrium could explain the large value of *a* found for cytochrome *c′* we computed the relaxation observables, T_1 and T_2, for the monomer and the dimer using the PDB structure 1rcp (Tahirov et al., 1996) with the consensus *a* value of 3.30 Å.

After filtering for flexibility and exchange, for each residue we computed the value of p_M that would reproduce the observed T_1/T_2. The mean value and the standard deviation for the 92 residues was 0.80 ± 0.04. Thus, we obtain the same population of monomer and dimer using independent data for each residue in spite of the completely different rotational diffusion tensors for the monomer and the dimer, and the different orientations of the equivalent N-H bonds in the two structures. At a concentration of 7 mM, this corresponds to a dissociation constant of 44.8 mM. Thus, in contrast to the barnase-barstar case, no detectable exchange contributions are expected. Experimental T_1/T_2 values are well reproduced using both the monomer structure (with $a = 4.35$ Å, Figure 3A) and the monomer-dimer model (with $a = 3.3$ Å, Figure 3B.

Under the monomer-dimer hypothesis, it is interesting that the relaxation data of cytochrome *c′* could be successfully used to refine the structure of the monomer. As the orientation of the individual molecules in the rotational diffusion tensors of the monomer and dimer is different (Figure 3C), the contribution of residues in the dimer to relaxation is not linearly correlated with those in the monomer. Thus, the contribution from the dimer, apart from scaling the correlation time, does not significantly affect the relative values of the relaxation parameters used as a source of structural information, and has the effect of an additional source of noise that does not prevent the refinement using the monomer structure.

Our calculations do not demonstrate the presence of monomer-dimer equilibrium, as deviations between the two models are within the experimental error of the experimental data (Figure 3D). However, the monomer-dimer equilibrium is compatible with all the available structural and relaxation data without the need to assume an unreasonable large hydration shell. Additionally, it proves the principle that, if such equilibrium exist, relaxation methods provide a very sensitive tool for its study and HYDRONMR can be used along with structural data of the monomer and dimer to estimate the corresponding equilibrium constant.

Both Titin module 128 and Antifungal protein 1 show larger than expected correlation times. In both cases, however the authors reported solubility problems and suggested the possibility of non-specific aggregation, although in the case of antifungal protein 1 no concentration dependent chemical shift changes were observed for the amide resonances for concentrations between 0.8 and 0.3 mM (Campos-Olivas et al., 2001).

From the previous examples we have seen that detecting aggregation may be difficult and some of the standard tests like dilution or measuring translational diffusion coefficients may fail in some cases. If the three-dimensional structure of the protein is known, we suggest that computation of the a value that best reproduces the experimental relaxation data using HYDRONMR provides a tool to cross-check relaxation and structural data and detect association processes.

Low values of the atomic element radius are less frequent in our survey and the absolute deviations from the average value are smaller than the ones observed in the opposite direction. The lowest values observed come from the study of two proteins containing two linked modules 127 and 128 of Titin. In one of the proteins the two modules were directly linked and in the second one the two modules were separated by a flexible Gly3 spacer (Improta et al., 1998). The structural model of the directly linked modules had been derived by placing the NMR structure of 127 and a homology model of 128, within the boundaries of the ellipsoids used to model small angle X-ray scattering data (Improta et al., 1996). In spite of the good agreement reported between calculated and experimental scattering data, NMR relaxation data could only be approximately reproduced with an *a* value of 2.15 Å for the construct with directly linked modules. Data from the more flexible construct could not be fitted even with an unnatural value of 2.0 Å. Thus, departures from the consensus *a* value may indicate deviations (static or dynamic) of the 3D structure from

the true structure in solution. A particular situation that is likely to be rather general is the presence of flexible tails that are assigned arbitrary coordinates in the structural models. This is the case of ubiquitin where using the complete X-ray structure (lubq) required an atomic element radius of 2.20 Å while removing the last three residues in the model allowed the simulation of the relaxation data with $a = 3.05$ Å. The same problem had been observed in previous hydrodynamic calculations of the same molecule (Tjandra et al., 1995).

HYDRONMR incorporates a complete treatment of anisotropic motion for a rigid body and it can be used to evaluate the effects of anisotropy in the relaxation times of individual ^{15}N residues. The extreme anisotropy of the 28 kDa Outer Surface Protein A (OspA) provides an interesting test of the performance of HYDRONMR. ^{15}N relaxation of OspA has been studied by the group of Nicholson (Pawley et al., 2001). Figure 4A shows that the large variations in T_1/T_2 values that appear in β-strands 5–13 are correctly predicted by HYDRONMR using the 18 Å resolution X-ray structure of OspA bound to a Fab fragment (Li et al., 1997). If the highly anisotropic motion of OspA was not considered, the relaxation data could have been interpreted as an evidence of extensive variations in the amplitude of motion in this region. On the other hand, two residues in the C terminal region (residues G218, I224) that have T_1/T_2 values comparable to those found in strands 5–13, cannot be explained on the basis of the anisotropic tumbling of the X-ray structure and may be affected by chemical exchange. Residue K210 in the same region shows also a large T_1/T_2 value but in this case HYDRONMR clearly shows that it is a consequence of the small angle of the corresponding NH vector with the principal axes of the rotational diffusion tensor. Anisotropy can also partially explain the large value of T_1/T_2 of residue E229, but an exchange contribution can not be discarded as the discrepancy between experimental and HYDRONMR calculated T_1/T_2 values exceeds the experimental uncertainty.

Thus, when a correct model is available, HYDRONMR allows a straightforward discrimination between anisotropy and chemical exchange that would otherwise require measurements at different magnetic fields or a comparison of longitudinal and transverse cross-correlation rates (Kroenke et al., 1998).

When just a few residues form a small angle with the main axis of the rotational diffusion tensor, discerning between exchange and anisotropy becomes crucial.

Dynamics of ribonuclease H has been exhaustively studied using NMR relaxation (Mandel et al., 1995, 1996; Yamasaki et al., 1995, 1999). Mandel et al., using only 37 T_1/T_2 values that fulfill the Tjandra et al. filtering protocol obtained a $D_{par}/D_{per} = 1.12 \pm 0.02$ (Mandel et al., 1996). ^{1}H-^{15}N/^{15}N CSA cross-correlation, η_{xy}/η_z measurements, that explicitly differentiate between anisotropy and exchange, made available 70 residues for the analysis of the diffusion tensor, yielding a much higher anisotropic model, $D_{par}/D_{per} = 1.23 \pm 0.02$. In this study residue W90 was unequivocally identified as being affected by exchange processes. On the other hand, residues V101 and L111 that had been excluded in the previous work because they did not fulfill Tjandra's protocol, were shown to be strongly affected by anisotropy motion. HYDRONMR calculations using the 2rn2 X-ray structure give a rotational diffusion tensor with $D_{par}/D_{per} = 1.24$ in good agreement with the refined experimental value. Figure 4B shows calculated and experimental values of T_1/T_2 along the sequence of ribonuclease H. T_1/T_2 values for V101 and L111, two of the largest calculated values in ribonuclease H, are 11.50 and 11.27 respectively, within experimental error of the values measured at 14.09 T: 11.71 ± 0.35 and 11.29 ± 0.65, respectively. On the other hand, for residue W90, at 11.74 T the experimental T_1/T_2 value is much larger than the calculated one: 8.62 ± 0.12 and 6.86, respectively, indicating a substantial contribution from exchange. A large discrepancy is also observed between experimental and calculated T_1/T_2 values for A51 and L59 in Figure 3B. Although cross-correlation rates (Kroenke et al., 1998) do not detect a large exchange effect for those residues, Mandel et al. (1996) observed a temperature dependence of the exchange term, R_{ex}, with the inverse of the temperature.

Those contradictory results could arise from the small, but real, contribution from exchange, as pointed out for other residues, e.g., K91 (Kroenke et al., 1998). Thus HYDRONMR calculations for individual residues are in agreement with the results of sophisticated experiments that allow the discrimination between exchange and anisotropy effects. Likewise, T_1/T_2 values lower than those predicted by HYDRONMR are usually associated to fast motions. This can be confirmed by the observation of low NOE values, as in the case of residue L60 of OspA (Figure 4A) that has a NOE value of just 0.51. Low T_1/T_2 values alone cannot be used as evidence for

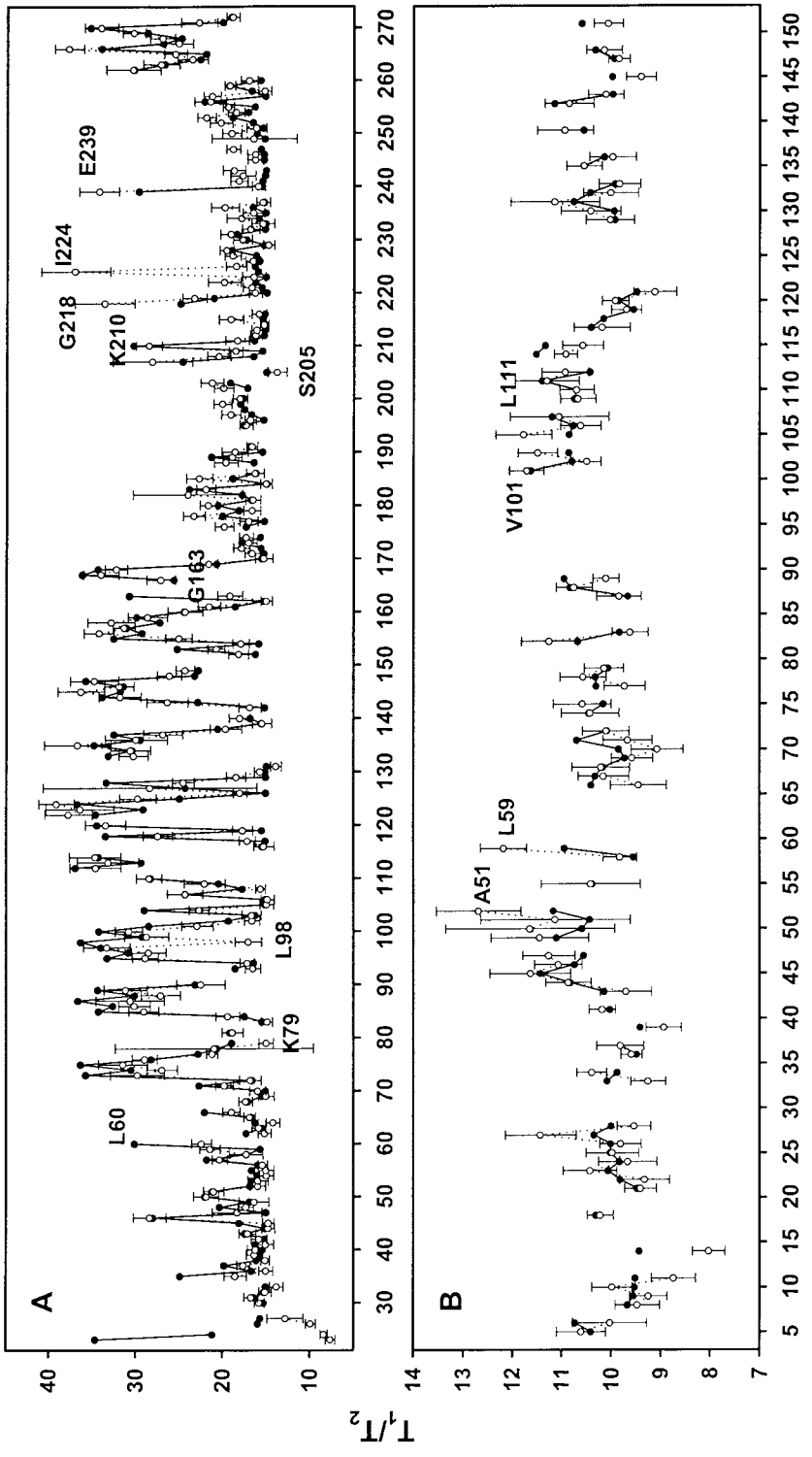

Figure 4. Experimental (open symbols, dotted line) and HYDRONMR (filled symbol, solid line) T_1/T_2 values along the sequence of (A) OspA and (B) Ribonuclease H at 14.1 T.

fast motion, as they could also correspond to a NH vector oriented orthogonal to the main axis of the diffusion tensor. Residues K79 and S205 exemplify this. Residue K79 shows evidence of fast local motion, with an NOE value of 0.58. On the other hand, S205 has no flexibility but shows a lower value of T_1/T_2 than K79. Flexibility cannot explain the large discrepancies between experimental and theoretical T_1/T_2 values for residues L98 and G163 as both residues present large values of NOE. A possible explanation could be some local difference between the X-ray and solution structures, maybe related to the presence of the Fab fragment, although these residues are not directed to the Fab-OspA interface.

Conclusions

HYDRONMR represents the state-of-the-art methodology for hydrodynamic modeling and allows the calculation of relaxation parameters from atomic scale structural models. HYDRONMR correctly reproduces experimental data for individual residues in proteins that behave as rigid bodies. This provides a very easy way to identify residues involved in exchange or fast local motions. The only adjustable parameter of HYDRONMR, the atomic element radius, is restricied to a narrow range for most proteins. Deviations towards large values is often associated to oligomerization or microaggregation processes while deviations to lower values seems to be associated to inappropriate models, possibly because of underlying large scale motions.

Computer programs

HYDRONMR can be downloaded, along with other components of the HYDRO suite of programs, from the website http://leonardo.fcu.um.es/macromol.

Acknowledgements

We thank A. Pastore, R. Campos-Olivas, R.V. Hosur and L. Nicholson for providing us unpublished relaxation data and M. Blackledge for useful discussions. Financial support by the Spanish Ministerio de Ciencia y Tecnología (BIO2001-3115, and BQU2000-0229), Generalitat de Catalunya and Ministerio de Educación y Cultura (predoctoral grant to P.B.) is gratefully acknowledged.

References

Akke, M., Brüschweiler, R. and Palmer, III, A.G. (1993) *J. Am. Chem. Soc.*, **115**, 9832–9833.
Blackledge, M., Cordier, F., Dosset and Marion, D. (1998) *J. Am. Chem. Soc.*, **120**, 4538–4539.
Campos-Olivas, R., Hörr, I., Bormann, C., Jung, G. and Gronenborn, A.M. (2001) *J. Mol. Biol.*, **308**, 765–782.
Carrasco, B. and García de la Torre, J. (1999) *Biophys. J.*, **76**, 3044–3057.
Case, D.A. (1999) *J. Biomol. NMR*, **15**, 95–102.
Cordier, F., Caffrey, M., Brutscher, B., Cusanovich, M.A., Marion, D. and Blackledge, M. (1998) *J. Mol. Biol*, **281**, 341–361.
Cusanovich, M.A. (1971) *Biochim. Biophys. Acta*, **236**, 238–241.
Dayie, K.T, Wagner, G. and Lefèvre, J.-F. (1996) *Annu. Rev. Phys. Chem.*, **47**, 243–282.
de Alba, E., Baber, J.L. and Tjandra, N. (1999) *J. Am. Chem. Soc.*, **121**, 4282–4283.
Feher, V.A. and Cavanagh, J. (1999) *Nature*, **400**, 289–293.
Fernandes, M.X., Bernadó, P., Pons, M. and García de la Torre, J. (2001) *J. Am. Chem. Soc.*, **123**, 12037–12047.
Fernandes, M.X., Ortega, A., López-Martínez, M.C. and García de la Torre, J. (2002) *Nucl. Acids Res.*, **30**, 1782–1788.
Filson, D.P. and Bloomfield, V.A. (1967) *Biochemistry*, **6**, 1650–1658.
Fischer, M.W.F., Majumdar, A. and Zuiderweg, E.R.P. (1998) *Prog. NMR Spectrosc.*, **33**, 207–272.
Fushman, D., Cahill, S. and Cowburn, D. (1997) *J. Mol. Biol.*, **266** 173–94.
Fushman, D., Ghose, R. and Cowburn, D. (2000) *J. Am. Chem. Soc.*, **122**, 10640–10649.
Gagné, S.M., Tsuda, S., Spyracopoulos, L., Kay, L.E. and Sykes, B.D. (1998) *J. Mol. Biol.*, **278**, 667–686.
García de la Torre, J. (2001) *Biophys. Chem.*, **93**, 159–170.
García de la Torre, J. and Bloomfield, V.A. (1977) *Biopolymers*, **16**, 1747–1763.
García de la Torre, J. and Bloomfield, V.A. (1981) *Quart. Rev. Biophys.*, **14**, 81–139.
García de la Torre, J., Huertas, M.L. and Carrasco, B. (2000a) *Biophys. J.*, **78**, 719–730.
García de la Torre, J., Huertas, M.L. and Carrasco, B. (2000b) *J. Magn. Reson.*, **147**, 138–146.
Improta, S., Krueger, J., Gautel, M., Atkinson, R.A., Lefèvre, J.-F., Moulton, S., Trewhella, J. and Pastore, A. (1998) *J. Mol. Biol.*, **284**, 761–777.
Improta, S., Politou, A.S. and Pastore, A. (1996) *Structure*, **4**, 323–337.
Korchuganov, D.S., Nolde, S.B., Reibarkh, M.Y., Orekhov, V.Y., Schulga, A.A., Ermolyuk, Y.S., Kirpichnikov, M.P. and Arseniev, A.S. (2001) *J. Am. Chem. Soc.*, **123**, 2068–2069.
Korzhev, D.M., Billeter, M., Arseniev, A.S. and Orekhov, V.Y. (2001) *Prog. NMR Spectrosc.*, **38**, 197–266.
Krishnan, V.V. and Cosman, M. (1998) *J. Biomol. NMR*, **12**, 177–182.
Kroenke, C.D., Loria, J.P., Lee, M., Rance, M. and Palmer, III, A.G. (1998) *J. Am. Chem. Soc.*, **120**, 7905–7915.
Kroenke, C.D., Rance, M. and Palmer, III, A.G. (1999) *J. Am. Chem. Soc.*, **121**, 1019–10125.
Li, H., Dunn, J.J., Luft, B.J. and Lawson, C.L. (1997) *Proc. Natl. Acad. Sci. USA*, **94**, 3584–3589.
Lipari, G. and Szabo, A. (1982) *J. Am. Chem. Soc.*, **104**, 4546–4559.
Mackay, J.P., Shaw, G.L. and King, G.F. (1996) *Biochemistry*, **35**, 4867–4877.

Mandel, A.M., Akke, M. and Palmer, III, A.G. (1995) *J. Mol. Biol.*, **246**, 144–163.
Mandel, A.M., Akke, M. and Palmer, III, A.G. (1996) *Biochemistry*, **35**, 16009–16023.
Mulder, F.A., Mittermaier, A., Hon, B., Dahlquist, F.W. and Kay, L.E. (2001) *Nat. Struct. Biol.*, **8**, 932–935.
Orekhov, Y.V., Nolde, D.E., Golovanov, A.P., Dorzhenev, D.M. and Arseniev, A.S. (1995) *Appl. Magn. Reson.*, **9**, 581–588.
Osborne, M.J. and Wright, P.E. (2001) *J. Biomol. NMR*, **19**, 209–230.
Palmer, III, A.G., Williams, J. and McDermott, A. (1996) *J. Phys. Chem.*, **100**, 13293–13310.
Pawley, N.H., Wang, C., Koide, S. and Nicholson, L.K. (2001) *J. Biomol. NMR*, **20**, 149–165.
Sahu, S.C., Bhuyan, A.K., Udgaonkar, J.B. and Hosur, R.V. (2000) *J. Biomol. NMR*, **18**, 107–118.
Spyracopoulos, L. and Sykes, B.D. (2001) *Curr. Opin. Struct. Biol.*, **11**, 555–559.
Tahirov, T.H., Shintaro, M., Meyer, T.E., Cusanovich, M., Higuchi, Y. and Yasuako, N. (1996) *J. Mol. Biol.*, **259**, 467–479.
Tjandra, N. and Bax, A. (1997) *Science*, **278**, 1111–1114.
Tjandra, N., Feller, S.E., Pastor, R.W. and Bax, A. (1995) *J. Am. Chem. Soc.*, **117**, 12562–12566.
Tjandra, N., Garrett, D.S., Gronenborn, A.M., Bax, A. and Clore, G.M. (1997) *Nat. Struct. Biol.*, **4**, 443–449.
Tjandra, N., Wingfield, P., Stahl, S. and Bax, A. (1996) *J. Biomol. NMR*, **8**, 273–284.
Tolman, J.R., Flanagan, J.M., Kennedy, M.A. and Prestegard, J.H. (1995) *Proc. Natl. Acad. Sci. USA*, **92**, 9279–9283.
Tsan, P., Hus, J.-C., Caffrey, M., Marion, D. and Blackledge, M. (2000) *J. Am. Chem. Soc.*, **122**, 5603–5612.
Wong, K.-B., Fersht, A.R. and Freund, S.M.V. (1997) *J. Mol. Biol.*, **268**, 494–511.
Yamasaki, K., Saito, M., Oobatake, M. and Kanaya, S. (1995) Biochemistry, **34**, 6587–6601.
Yang, D. and Kay, L.E. (1996) *J. Mol. Biol.*, **263**, 369–382.
Zweckstetter, M. and Bax, A. (2000) *J. Am. Chem. Soc.*, **122**, 3791–3792.